Appendix III: The Identification of haematite as the colouring agent in red ochre from the Middie Palaeolithic Site C at Maas-tricht-Belvédère, The Netherlands, by means of x-ray diffraction analysis

Arps, C.E.S.

Citation

Arps, C. E. S. (1988). Appendix III: The Identification of haematite as the colouring agent in red ochre from the Middie Palaeolithic Site C at Maas-tricht-Belvédère, The Netherlands, by means of x-ray diffraction analysis. In *Analecta Praehistorica Leidensia 21 : From find scatters to early hominid behavior: A study of middle palaeolithic riverside settlements at Maastricht-Belvédère (The Netherlands)* (Vol. 21, pp. 163-166). Leiden University Press. Retrieved from https://hdl.handle.net/1887/27932

C.E.S. Arps[1]

appendix III

The identification of haematite as the colouring agent in red ochre from the Middle Palaeolithic Site C at Maastricht-Belvédère, The Netherlands, by means of x-ray diffraction analysis

In the course of the excavations carried out by the Institute of Prehistory, 14 crusty pieces of reddish material, ranging in diameter from about 0.4 to 1.5 cm, were collected from the sandy deposits at Site C. The constrast between the red material and the yellowish-brown (2.5 Y 5/3) to greyish-olive (5 Y 5/3) sediment and the crusty character of the concentrate made recovery of the tiny and fragile fragments possible. Three samples were submitted to our museum by the excavator (W. Roebroeks) for analysis of the red stain (fig. 154).

A granulometric analysis (fig. 155) showed the sedimentary rock to be a reasonably- to well-sorted finely to very finely-grained quartz sand with a silt and clay content of up to 15% by weight. The grain-shapes vary from sub-angular or angular (the majority) to well-rounded. A binocular microscopic investigation of the red concentrate revealed that the staining agent surrounded the larger quartz grains as a very thin coating or had clotted together with the silt and clay particles. Individual reddish crystal grains, e.g.haematite, were not visible.

The main part of the red crusty material (fig. 154) was sampled and carefully ground in order to release the reddish powder, but at the same time care was taken to avoid breaking the quartz grains. The sample was placed in a concave glass dish filled with alcohol and the finest fraction of the reddish powder could be separated from the bulk sample by panning. This concentrate required further grinding to obtain a suitable grain-size for the production of a distinct X-ray diffraction pattern.

Using a Debeye-Scherrer powder camera (Philips PW 1024) with a diameter of 114.6 mm (fig. 156) and Fe-radiation and X-ray powder diffraction, a photograph was made, in which, by comparison with 'standard' photographs, only the presence of quartz could be detected. This museum's routine technique for mineral identification did not reveal the presence of a mineral phase that could be held responsible for the reddish stain of the investigated sample.

Determined to solve the problem, we carried out another experiment. This time the separated very finely-grained concentration was sent to the X-ray laboratory of the Institute of Earth Sciences, State University of Utrecht (Dr W.M.M. Heijnen). In this laboratory a special powder diffraction camera (fig. 156) is employed, viz. the Guinier-De Wolff Quadruple Focussing Camera (Enraf Nonius, Delft), with which diffraction angles of extremely high

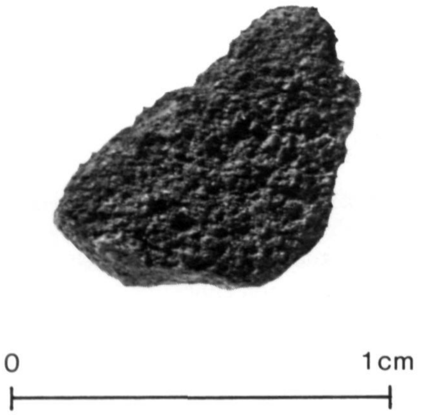

Fig. 154. Haematite-concretion Bv-894. The scale bar measures 1 cm.

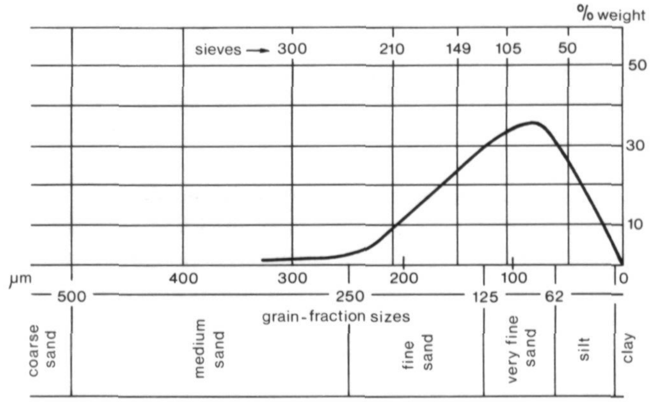

Fig. 155. Grain-size distribution of the sediment in which the Site C haematite-concretions were found.

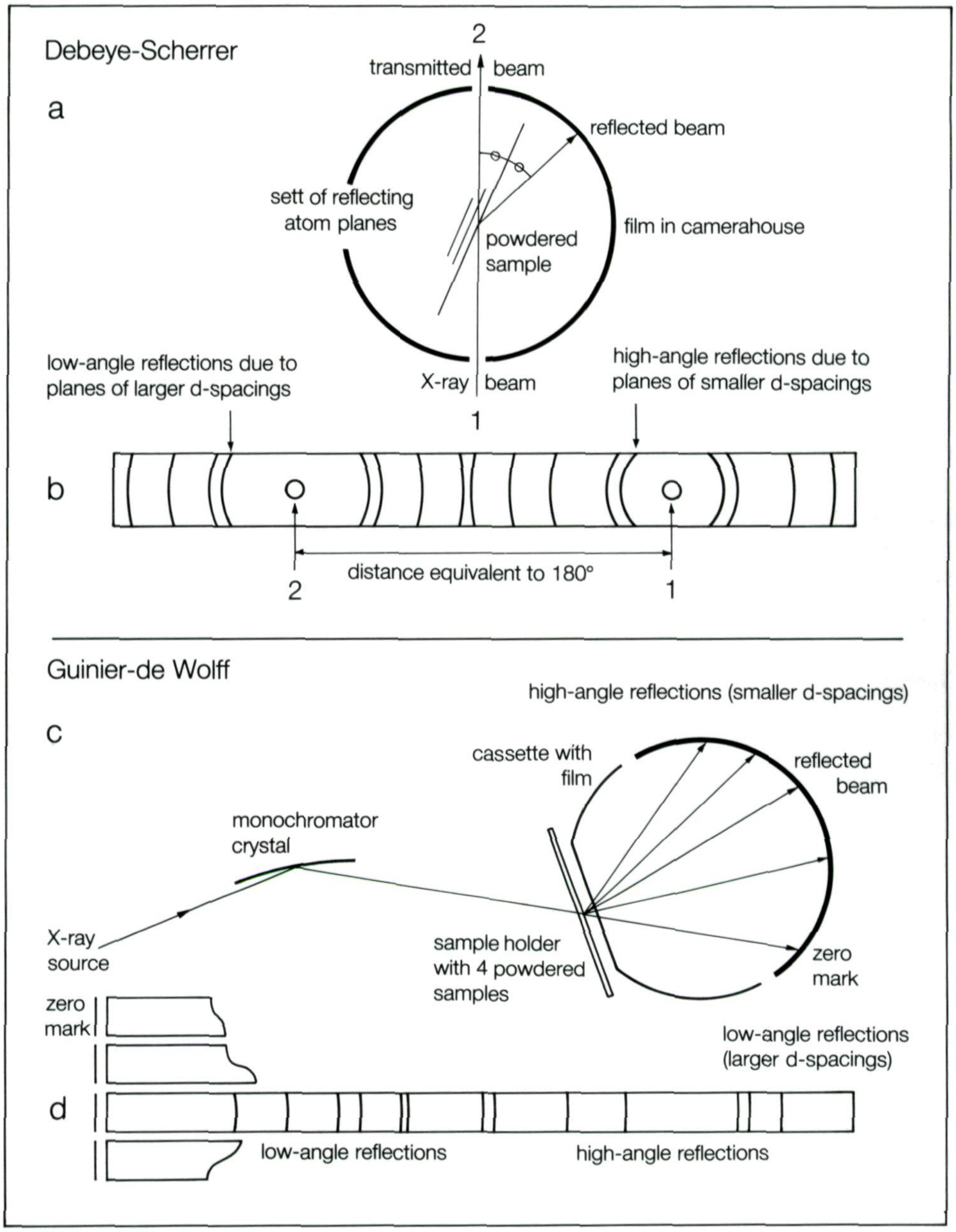

Fig. 156. X-ray powder diffraction data as can be obtained with a Debeye-Scherrer and a Guinier-De Wolff camera.

precision can be obtained. The dispersion of this camera is equivalent to that of a 229.2-mm Debeye-Scherrer camera. This time an X-ray tube producing Cu(KoC)-radiation was used. Exposure time was set at 2.5 hours with an X-ray intensity of 40 kV and 20 mA. Figure 157 is the result obtained after the development of the exposed film. It (again) clearly shows the quartz diffraction lines, but also reveals the presence of a number of additional weak lines. A millimetre scale was used to measure the distance between the lines and the zero-mark (incident beam). The dispersion constant was 4 mm per degree of the diffraction angle.

From the diffraction angles the so-called interplanar spacings, i.e. the distances between the planes of atoms in a crystal lattice, also known as d-spacings, can be calculated. For this purpose conversion tables are used, e.g. that of the National Bureau of Standards, Applied Mathematical Series 10, 1950 (USA). Each mineral is characterized by a series of specific d-values with different intensities. In figure 157 the main diffraction lines of quartz are clearly visible. The d-values of the strongest lines have been indicated. The few weak extra lines were identified as representing the main characteristic line of haematite (alpha-Fe_2O_3). But the

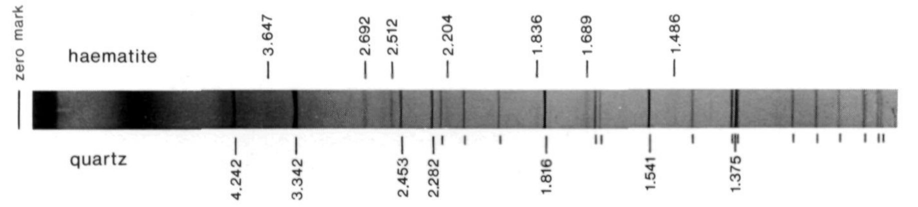

Fig. 157. X-ray diffraction data obtained with sample D23/16, indicating the mixture of quartz and haematite.

relative intensities of these lines could hardly be estimated. The haematite lines are also indicated in fig. 157, together with their d-values. In table 32 the complete set of visible d-values of quartz and haematite are listed and compared with values from the literature (Joint Committee on Powder Diffraction Standards, 1974). The values of goethite, alpha-Fe_3^+ O(OH), are added for comparison, although this iron hydroxide mineral cannot be held responsible for the red stains in the sand deposit of the Belvédère prehistoric site.

From the X-ray analysis it can therefore be concluded that the 'red ochre' stain was caused by the presence of haematite.

note

[1] National Museum of Geology and Mineralogy, Leiden, the Netherlands

Table 32

QUARTZ				HAEMATITE				GOETHITE	
J.C.P.D.S.	Belvédère	J.C.P.D.S.	Belvédère	J.C.P.D.S.					
d	I	d	I	d	I	d	I	d	I
4.26	35	4.242	40					4.98	10
3.343	100	3.342	100					4.18	100
2.458	12	2.453	30	3.66	25	3.674	w		
2.282	12	2.282	30					3.38	10
2.237	6	2.236	15	2.69	100	2.69	r	2.69	30
2.128	9	2.127	20					2.58	8
1.980	6	1.977	15	2.51	50	2.512	rg		
1.817	17	1.816	40					2.49	16
1.672	7	1.671	15					2.452	25
1.659	3	1.658	10					2.252	10
1.608	<1			2.201	30	2.204	w		
1.541	15	1.541	30					2.192	20
1.453	3	1.451	10	1.838	40	1.836	w		
1.418	<1							1.799	8
1.382	7	1.382	15					1.721	20
1.375	11	1.375	30	1.690	60	1.689	r	1.694	10
1.372	9	1.372	15	1.596	16	1.595	w	1.564	16
1.288	3	1.287	10					1.509	10
1.256	4	1.255	10	1.484	35	1.486	w		
1.228	2	1.226	5	1.452	35			1.453	10
1.1997	5	1.196	10					1.392	8
1.1973	2	1.195	w					1.357	8
1.1838	4	1.180	5					1.317	8
1.1802	4	1.176	5	1.310	20				
1.1530	2			1.258	8				
1.0816	4			1.189	8				
				1.162	10				
				1.141	12				
				1.102	14				

d: interplanar spacings
I: intensity of reflection
w: weak, r: reasonable, rg: reasonably good